Quantum Electronics **45** (11) 1069–1074 (2015)

RADIATION SCATTERING

PACS numbers: 42.25.Fx; 87.64.Cc
DOI: 10.1070/QE2015v045n11ABEH015824

Control of optical transport parameters of 'porous medium–supercritical fluid' systems

D.A. Zimnyakov, O.V. Ushakova, S.A. Yuvchenko, V.N. Bagratashvili

Abstract. **The possibility of controlling optical transport parameters (in particular, transport scattering coefficient) of porous systems based on polymer fibres, saturated with carbon dioxide in different phase states (gaseous, liquid and supercritical) has been experimentally studied. An increase in the pressure of the saturating medium leads to a rise of its refractive index and, correspondingly, the diffuse-transmission coefficient of the system due to the decrease in the transport scattering coefficient. It is shown that, in the case of subcritical saturating carbon dioxide, the small-angle diffuse transmission of probed porous layers at pressures close to the saturated vapour pressure is determined by the effect of capillary condensation in pores. The immersion effect in 'porous medium–supercritical fluid' systems, where the fluid pressure is used as a control parameter, is considered. The results of reconstructing the values of transport scattering coefficient of probed layers for different refractive indices of a saturating fluid are presented.**

Keywords: *immersion effect, porous systems, diffuse transmission, supercritical fluid, transport scattering coefficient.*

1. Introduction

The effect of scattering suppression in multiphase microstructured systems with matched refractive indices of different structural components (the immersion effect) has been known for a very long time; however, it was systematically studied and described for the first time by Christiansen at the end of the XIX century. In the middle of the XX century, the interest in the immersion effect in dispersed systems was related to the possibility of designing dispersion filters for visible and mid-IR ranges on their basis (see, e.g., [1, 2]). However, a number of fundamental limitations, related to the difficulties in fitting their components and strong influence of external factors (in particular, temperature) on the parameters of filters restricted their application. At the same time, controlled optical devices with a dispersed structure can be designed based on specifically this influence.

Currently, the interest in the immersion control of optical properties of randomly inhomogeneous media is caused to a great extent by the possibility of increasing the biological-tissue probing depth in optical microscopy and optical coherence tomography [3–6]. An increase in the probe beam transport length l^* and scattering length l_s [7] in a biological tissue saturated by a biologically compatible immersion agent makes it possible to visualize fabric structures at larger depths in comparison with a natural tissue.

Note also that the immersion effect in layers of close-packed scattering particles or porous media saturated by a liquid with a large refractive index is successfully applied to study the specific features of radiation transfer when the transport length l^* is comparable with the light wavelength λ, and the optical parameters of the medium should be affected by local interference effects on the scale of wavelength λ [8].

In randomly inhomogeneous dispersed media, which are disordered ensembles of scattering particles immersed in a homogeneous matrix medium, replacement of the matrix medium with an immersion agent is generally implemented via diffusion or capillary transport of this agent from the surface to the volume probed. Under these conditions, it is rather difficult to estimate quantitatively the change in the refractive index n_m of the matrix medium as a result of immersion. In addition, the main methods that are currently used to control the n_m value in an experiment are based on changing either the volume fraction of the immersion agent in the matrix medium or the temperature of the system. Along with the difficulties in quantitative estimation of the n_m value, a significant drawback of these techniques is their inertia, which is related to long characteristic times of attaining equilibrium. When the temperature factor is used, the possibility of controlling the matrix refractive index is often limited by the small value of the corresponding temperature coefficient.

In this study, we consider another approach to optical immersion of dispersed media, which is based on application of supercritical fluids with controlled density as immersion agents. Naturally, this approach cannot be used to solve biomedical problems implying optical clearing of biological tissues. However, it may be efficient in analysis of structural and optical properties of systems of consolidated and nonconsolidated micro- and nanoparticles in physical materials science, because in this case the n_m value can easily be controlled in a wide range. In addition, the study of the relationship between the optical properties of dispersed systems possessing super-

D.A. Zimnyakov, O.V. Ushakova, S.A. Yuvchenko Yuri Gagarin State Technical University of Saratov, ul. Politekhnicheskaya 77, 410054 Saratov, Russia;
e-mail: zimnykov@mail.ru, s_sov@rambler.ru, yuv-sergej@yandex.ru;
V.N. Bagratashvili Institute on Laser and Information Technologies, Russian Academy of Sciences, Pionerskaya ul. 2, Troitsk, 142190 Moscow, Russia; M.V. Lomonosov Moscow State University, Vorob'evy gory, 119991 Moscow, Russia;
e-mail: victor.bagratashvili@gmail.com

Received 31 March 2015; revision received 2 June 2015
Kvantovaya Elektronika **45** (11) 1069–1074 (2015)
Translated by Yu.P. Sin'kov

critical fluid components and the processes of interaction of supercritical fluids with condensed media under spatial limitation is of certain interest for developing optical methods of diagnostics in rapidly developing supercritical fluid technologies. Note that the number of studies on the optical diagnostics of multiphase systems with subcritical and supercritical fluids is rather limited. One of possible approaches in this field is coherent anti-Stokes Raman scattering (CARS) spectroscopy, which is used to analyse the specific features of the fluid behaviour in nanopores near the critical point [9–11]; however, this approach is fit for only transparent porous media (for example, nanoporous glass Vycor) and cannot be applied to dispersed systems with large scattering coefficients. In this case, one can successfully use full-field speckle correlometry, which, in particular, made it possible to reveal specific features of capillary condensation in porous media and their relaxation dynamics near the saturating-component critical point [12–14]. In our case, the immersion effect in porous media saturated with carbon dioxide under isothermal change in pressure was investigated based on changes in the small-angle diffuse transmission of a laser beam by a layer of medium.

2. Experimental technique and results

We experimentally investigated the dependence of the small-angle diffuse transmission of different porous layers with fibrillar structure on the pressure of saturating carbon dioxide. The experiments were performed in the isothermal mode at different temperatures near the carbon dioxide critical point ($T_{cr} \approx 304.1282$ K). The objects of study were layers of F-type filter paper [GOST (State Standard) 12026-76] and sealing polytetrafluoroethylene (PTFE) ribbon with a pronounced fibrous structure (FUM-2, technical specifications 6-05-1388-8); the sample thickness was $L \approx 100 \pm 5$ μm in both cases. A schematic diagram of the experimental setup is shown in Fig. 1. Samples were placed in high-pressure stainless steel optical cell (*15*) with sapphire windows so as to be oriented perpendicular to the propagating direction of the beam of He–Ne laser (*10*) (GN-5P, $\lambda = 633$ nm, output power 5 mW, linear polarisation). The cell was filled with carbon dioxide through a high-pressure capillary; a desired pressure in the cell was set manually using high-pressure plunger pump (*6*). We performed experiments with both passive thermal stabilisation (using a heat-insulating foam plastic jacket) and active thermal stabilisation of the cell [using heater (*8*) containing a complementary pair of high-power transistors and temperature sensor (*12*) based on a quartz generator (the cell temperature was determined from the generator frequency deviation from the nominal value)]. The stabilisation system provided rms temperature fluctuations with respect to a specified value in the operating range (293–307 K) of no more than 0.01 K. Laser radiation, scattered by probed layers forward at small angles with respect to the incident beam was recorded for different carbon dioxide pressures in the cell. The pressure changed from atmospheric to 10 MPa with a step of 0.2 MPa; the relative error in measuring pressure was 1%.

The radiation scattered forward into small angles was recorded by a monochromatic Thorlabs DCC1545M CMOS camera (1280 × 1024 pixels, pixel size 5.2 × 5.2 μm, quantum efficiency about 0.52 at a wavelength of 633 nm) without an

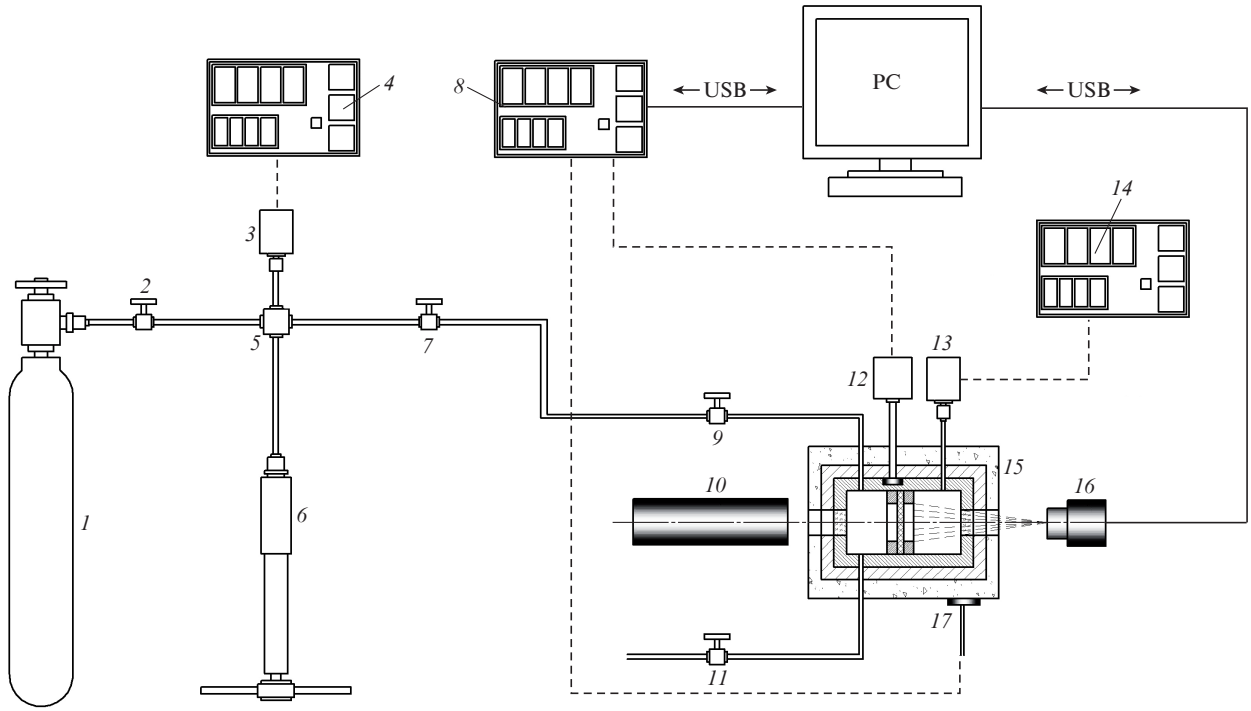

Figure 1. Schematic of the experimental setup: (*1*) balloon with carbon dioxide; (*2*, *7*) high-pressure valves; (*3*, *13*) pressure sensors; (*4*) pressure indicator in the high-pressure line; (*5*) four-way valve; (*6*) manual high-pressure pump; (*8*) temperature indicator–controller for high-pressure optical cell; (*9*) inlet high-pressure valve; (10) laser; (*11*) outlet high-pressure valve; (*12*) sensor of cell temperature; (*14*) indicator of cell pressure; (*15*) high-pressure optical cell; (*16*) CMOS camera; (*17*) cell heater.

objective; the camera was installed at a distance of 65 mm from the probed layer, coaxially with the probe beam. The area of the CMOS matrix used to calculate the average intensity of forward-scattered radiation, was 120 × 120 pixels. Before the measurements, we calibrated the camera using a set of neutral light filters with known optical densities; the intensity of the laser beam transmitted through the cell containing no samples but only carbon dioxide under atmospheric pressure was recorded. Calibration was performed using different combinations of neutral light filters from a set of standards KNF-1M (State Register, No. 37858–08) and a Gentec Maestro laser power meter.

Figure 2 shows the dependences of normalised laser beam intensity $\tilde{I}$ (small-angle diffuse transmission coefficient), scattered by probed samples at small ($\theta \leqslant 5.3$ mrad) angles, on the carbon dioxide pressure in the cell. The intensity values were normalised to the laser beam intensity transmitted through the cell without sample. Curves (*1*) and (*3*) correspond to the subcritical temperature of the gas in the cell, whereas curves (*2*) and (*4*) were obtained at $T > T_{cr}$. We also measured (using Thorlabs IS236A-4 integrating spheres) the diffuse-transmission and reflection coefficients (T_{dif} and R_{dif}, respectively) of the porous layers under study in air at room temperature ($\lambda = 633$ nm). Based on the measured values, the scattering coefficient μ_{s633} and transport scattering coefficient μ'_{s633} were reconstructed by inverse Monte Carlo simulation; they turned out to be, respectively, 108 and 65 mm^{-1} for filter paper layers and 117 and 48 mm^{-1} for PTFE ribbon layers. Note that the $\mu_{s633}L$ values for both the paper and PTFE ribbon samples significantly exceed unity and are approximately 10.8 (for filter paper) and 11.7 (for PTFE ribbon). This fact is indicative of almost complete suppression of the unscattered ('coherent') component of the laser beam emerging from the probed layers.

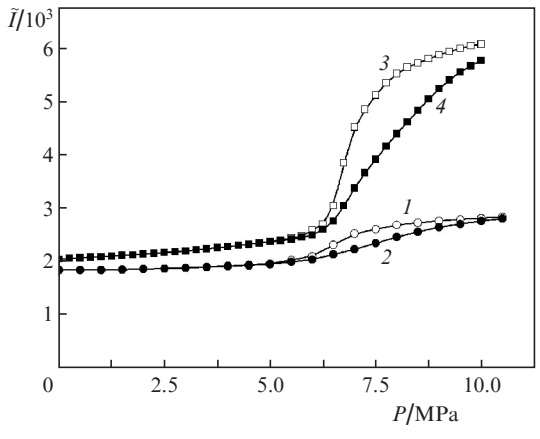

Figure 2. Experimental dependences of the small-angle diffuse transmission coefficient of porous layers on the saturating-agent pressure for (*1*, *3*) subcritical carbon dioxide ($T = 301.16$ K) and (*2*, *4*) supercritical carbon dioxide ($T = 306.16$ K); the probed media are layers of (*1*, *2*) filter paper and (*3*, *4*) PTFE ribbon.

3. Results and discussion

The increase in $\tilde{I}$ with an increase in carbon dioxide pressure is due to the increase in the density (and, correspondingly, refractive index) of the medium saturating porous layers. Note a characteristic feature in the dependences $\tilde{I}(P)$ (observed at $T < T_{cr}$): there is no jump of small-angle diffuse transmission of probed layers at the pressure in the cell corresponding to saturated vapour pressure P_{sat} at a specified temperature. The fast but sufficiently smooth increase in $\tilde{I}$ with an increase in pressure at $P < P_{sat}$ is due to the capillary condensation of carbon dioxide in pores [15], which leads to coexistence of the liquid and gaseous phases in the ensemble of pores at pressures below the saturated vapour pressure. An increase in pressure is accompanied by gradual filling of pores with the liquid phase. The liquid-phase volume fraction f in the pore ensemble tends to 1.0 at $P \to P_{sat}$. The effective refractive index of the porous three-phase system, matrix–gas–liquid, as a function of the thermodynamic parameters of the saturating medium with pores much smaller than the light wavelength in size can be estimated using the Maxwell Garnett or Bruggeman effective-medium models [16]. However, these calculations, in which the shape of pores must be taken into account, are beyond the scope of this study. In qualitative analysis of the experimental data obtained at temperatures below the carbon dioxide critical temperature, the liquid-phase volume fraction f in the pores, which is formed due to the capillary condensation, can be estimated using the Kelvin model [15] with allowance for the pore size distribution. The permittivities (and, correspondingly, refractive indices) of the liquid and gaseous phases at specified densities can be determined using the modified Clausius–Mossotti relation, which, according to [17], adequately describes the behaviour of the permittivities of different media in both gaseous and liquid phases and in the supercritical state:

$$n_{liq,g,s} \approx \sqrt{\frac{1 + 2A\rho_{liq,g,s}}{1 - A\rho_{liq,g,s}}}, \qquad (1)$$

where the subscripts liq, g, and s denote, respectively, the liquid and gaseous phases and the supercritical state of the saturating medium. The experimentally found A value for carbon dioxide is $(1.42 \pm 0.012) \times 10^{-4}$ m^3 kg^{-1} [17]. To determine the carbon dioxide density in different states (liquid, gaseous and supercritical) as a function of temperature and pressure, one can use the online calculator of thermodynamic parameters of liquid, gaseous and supercritical media [18].

Note that the 'low-frequency' Maxwell Garnett or Bruggeman models can be used to estimate quantitatively the effective refractive index of the 'porous matrix–saturating medium' system below the critical point in the case of porous systems with an average pore size $\langle r \rangle$ much smaller than the probe light wavelength λ. At $\langle r \rangle \sim \lambda$, one should use other approaches to estimation of the effective refractive index of the saturating medium (for example, the effective-medium model described in [19]).

Figure 3 shows the dependences of the refractive index n_s of the saturating medium (supercritical carbon dioxide) on pressure P, calculated for the range $T > T_{cr}$ using Eqn (1) and the data on the density of supercritical CO_2 at specified T and P values, obtained with the calculator [18]. Under this condition, the problem of determining n_s is much simpler than in the case $T < T_{cr}$ due to the absence of coexistence of condensed and gaseous phases in the system of pores.

It is of interest to compare the optical clearing efficiencies of experimentally investigated randomly inhomogeneous

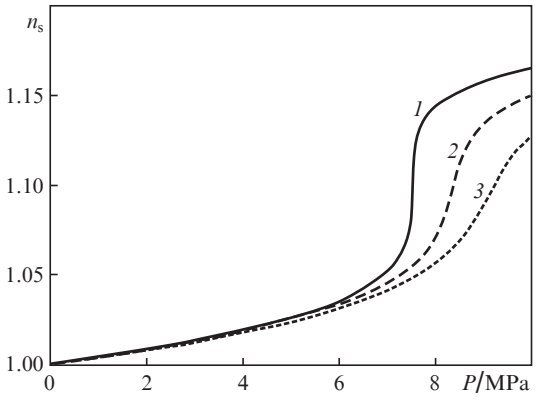

Figure 3. Theoretical pressure dependences of the refractive index of supercritical carbon dioxide, saturating the porous matrices under study, at T = (*1*) 305, (*2*) 310, and (*3*) 315 K.

porous media with a supercritical fluid (in particular, carbon dioxide) as an immersion agent. To this end, the transport scattering coefficient μ_s' of probed layers was reconstructed for different values of the refractive index of supercritical carbon dioxide saturating porous layers. The transport scattering coefficient $\mu_s' = 1/l^* = (1-g)/l = \mu_s(1-g)$ (g is the scattering anisotropy parameter and μ_s is the scattering coefficient of the medium [7]) is one of the main (along with the scattering anisotropy parameter) characteristics that control the probe light transport in weakly absorbing randomly inhomogeneous media. Correspondingly, the μ_s' value determines the ratio between the diffusively scattered and unscattered ('coherent') light-beam components in the forward-scattering mode. The μ_s' values were reconstructed using inverse Monte Carlo simulation on the assumption that variations in the refractive index of the saturating medium affect only slightly the scattering anisotropy parameter of probe light. This assumption appears to be justified, because simulation of the influence of n_s on the optical parameters of disordered systems of spheroidal scattering centres, performed with the aid of the online calculator [20], showed high sensitivity of the scattering efficiency factor Q_{sca} [16] and, correspondingly, lower sensitivity of g to changes in the refractive index of the matrix medium with particles. The refractive indices n of scatterers, in correspondence with the data of several publications and manufacturer's specifications, were taken to be 1.52 (for cellulose) and 1.35 (for polytetrafluoroethylene) in the simulation; the scattering of probe light with $\lambda = 633$ nm from systems of both nanosized ($g \approx 0$) and submicron ($g \approx 0.6$) scatterers was considered. The simulation results are presented in Fig. 4. For the systems of nanoscatterers, the n_s value barely affects the factor $1-g$, which enters the expression for μ_s' [Fig. 4a, curves (*1*), (*2*)], whereas for the systems of submicron particles the factor $1-g$ decreases with an increase in n_s. However, the influence of n_s on the scattering efficiency is much more pronounced for both the systems with isotropic scattering ($g \approx 0$) and the systems with the scattering anisotropy parameter ~0.6 (Fig. 4b).

Despite the possible significant differences of the effective scatterer shape from spheroidal in real probed systems, the conclusion (based on the simulation results) about the dominant influence of n_s on Q_{sca} and, to a smaller extent, g

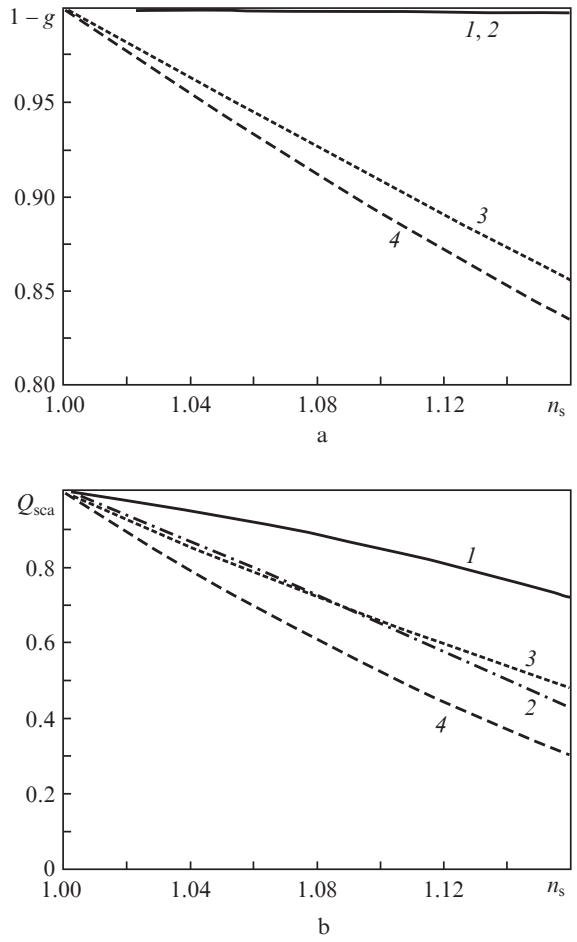

Figure 4. Theoretical dependences of the normalised values of the (a) parameter $1-g$ and (b) scattering efficiency factor Q_{sca} for model systems of spheroidal nanoparticles and submicron particles on the refractive index of the matrix medium containing (*1*) nanoparticles with an average size of 50 nm and a refractive index of 1.52, (*2*) nanoparticles with an average size of 50 nm and a refractive index of 1.35, (*3*) submicron particles with an average size of 350 nm and a refractive index of 1.52, and (*4*) submicron particles with an average size of 350 nm and a refractive index of 1.35. Parameters $1-g$ and Q_{sca} are normalised to their values at $n_s = 1$.

for disordered ensembles of scatterers with relatively low scattering anisotropy is fairly general and can be used to reconstruct μ_s' values. The reconstruction procedure was as follows: the small-angle diffuse transmission coefficient $\tilde{I}$ for the detection geometry used in our experiments was determined (by the direct Monte Carlo simulation) for the initial μ_s' value at specified values of g, effective refractive index, and geometric thickness of the layer. The simulation procedure was similar to that described in [14]. When the $\tilde{I}$ value was obtained, the residual between the calculated and measured values of the small-angle diffusion transmission coefficient was calculated and then minimised in a sequence of iterations by varying μ_s', with application of the Levenberg–Marquardt algorithm. We used the values of μ_s' and $g = 1 - \mu_s'/\mu_s$ derived from the experimental data on the diffuse transmission and reflection of probed layers at a wavelength of 633 nm as the initial values for the iterative procedure. The effective refractive index of probed layers at a specified n_s value, determined by the pressure of

supercritical carbon dioxide in the optical cell (Fig. 4a), was estimated within the Maxwell Garnett model (the volume fraction of pores in the layers was found from volumetric measurements). The refractive indices of porous matrix media were taken to be approximately equal to 1.52 for the paper samples and 1.34 for the PTFE ribbon samples.

Figure 5 shows the reconstructed values of transport scattering coefficient μ_s' at different refractive indices n_s of the saturating fluid. Note that the variability of μ_s' values in the working range of pressures (and, correspondingly, n_s values) for the PTFE ribbon samples is much higher than that for the paper samples: the transport scattering coefficient for the PTFE ribbon changes by a factor of more than 2, whereas the corresponding change for paper – by 40%. This difference is related to the lower refractive index of PTFE structural elements (fibres) in comparison with cellulose fibres. An analysis of the influence of the refractive index n_s of the matrix medium for disordered ensembles of spherical dielectric particles with g values corresponding to the systems under study showed that, in the used range of variation in n_s for particles with refractive indices of 1.52–1.55, the scattering efficiency factor changes by no more than a factor of 1.4–1.8. At the same time, for particles with refractive indices of 1.31–1.38, the scattering efficiency factor changes by a factor of more than 2.5 (Fig. 4b); this behaviour is in satisfactory agreement with the experimental data on the efficiency of optical clearing of porous media with application of supercritical carbon dioxide as an immersion agent.

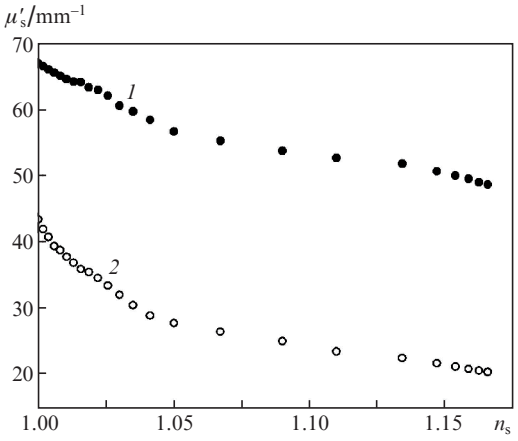

Figure 5. Dependences of the transport scattering coefficient of porous layers of (*1*) filter paper and (*2*) PTFE ribbon on the refractive index of saturating supercritical carbon dioxide [results of reconstruction from the experimental data in Fig. 2 (curves *2*, *4*) using inverse Monte Carlo simulation].

4. Conclusions

Thus, the experimental study of the immersion effect in porous systems saturated with carbon dioxide in the gaseous phase or in the supercritical state demonstrated a rather high efficiency of optical clearing of randomly inhomogeneous media using supercritical fluids as immersion agents. This approach has evident advantages as compared to the refractive index tuning (RIT) [21], which is based on controlling the refractive index of saturating gaseous phase by changing pressure. This advantage is related to a much higher variability of the saturating-substance refractive index in the case of supercritical fluids. At the same time, the analysis of the small-angle diffuse transmission of porous layers in the subcritical region as a function of pressure (under conditions of capillary condensation) can be used as a basis for characterising structural parameters of porous systems.

Acknowledgements. This work was supported by the Russian Scientific Foundation (Grant No. 14-33-00017) (the part related to the development and fabrication of a laboratory experimental setup) and the Russian Foundation for Basic Research (Grant No. 13-02-12092) (the part related to the experimental study of the diffuse transmission of 'porous medium–supercritical fluid' systems). D.A. Zimnyakov acknowledges the support of the Ministry of Education and Science of the Russian Federation in the part of the work related to the development of the algorithm and special software for inverse Monte Carlo simulation (within the basic part of the state contract for implementation of research in higher educational institutions). O.V. Ushakova acknowledges the support of the Ministry of Education and Science of the Russian Federation in the part of the work related to the development of the algorithms and special software for collecting and processing experimental data (Grant No. 14. Z56.15.7102-MK).

References

1. Borisevich N.A., Vereshchagin V.G., Validov M.A. *Infrakrasnye fil'try* (IR Filters) (Minsk: Nauka i Tekhnika, 1971).
2. Dik V.P., Loiko V.A. *Opt. Zh.*, **79** (7), 29 (2012).
3. Tuchin V.V., Xu X.Q., Wang R.K. *Appl. Opt.*, **41** (1), 258 (2002).
4. Tuchin V.V., Zhestkov D.M., Bashkatov A.N., Genina E.A. *Opt. Express*, **12** (13), 2966 (2004).
5. Tuchin V.V. *J. Phys. D Appl. Phys.*, **38** (15), 2497 (2005).
6. Zhu D., Larin K.V., Luo Q.M., Tuchin V.V. *Laser Photonics Rev.*, **7** (5), 732 (2013).
7. Ishimaru A. *Wave Propagation and Scattering in Random Media* (San Diego, California: Academic Press, 1978) Vol. 1.
8. Schuurmans F.J.P., Megens M., Vanmaekelbergh D., Lagendijk A. *Phys. Rev. Lett.*, **83** (11), 2183 (1999).
9. Arakcheev V.G., Morozov V.B. *Pis'ma Zh. Eksp. Teor. Fiz.*, **90** (7), 574 (2009).
10. Andreeva O.V., Arakcheev V.G., Bagratashvili V.N., Morozov V.B., Popov V.K., Valeev A.A. *J. Raman Spectroscopy*, **42** (9), 1747 (2011).
11. Arakcheev V.G., Morozov V.B. *J. Raman Spectroscopy*, **44** (10), 1363 (2013).
12. Zimnyakov D.A., Chekmasov S.P., Ushakova O.V., Bagratashvili V.N. *Sverkhkrit. Flyuidy: Teor. Prakt.*, **2**, 27 (2014).
13. Zimnyakov D.A., Chekmasov S.P., Sviridov A.P., Ushakova O.V., Bagratashvili V.N. *Sverkhkrit. Flyuidy: Teor. Prakt.*, **3**, 56 (2014).
14. Zimnyakov D.A., Chekmasov S.P., Ushakova O.V., Isaeva E.A., Bagratashvili V.N., Yermolenko S.B. *Appl. Opt.*, **53** (10), B12 (2014).
15. Gregg S.J., Sing K.S.W. *Adsorption, Surface Area, and Porosity* (Academic: London, 1982; Mir: Moscow, 1984) p. 157.
16. Bohren C.F, Huffman D.R. *Absorption and scattering of light by small particles* (Wiley: New York, 1983; Mir: Moscow, 1986).
17. Avdeev M.V., Konovalov A.N., Bagratashvili V.N., Popov V.K., Tsypina S.I., Sokolova M., Jie Ke, Poliakoff M. *Phys. Chem. Chem. Phys.*, **6**, 1258 (2004).
18. http://webbook.nist.gov/chemistry/fluid.

19. Zimnyakov D.A., Yuvchenko S.A., Sina Dzh. S., Ushakova O.V. *Pis'ma Zh. Eksp. Teor. Fiz*., **98** (6), 366 (2013).
20. http://omlc.org/calc/mie_calc.html.
21. Faez S., Johnson P.M., Lagendijk A. *Phys. Rev. Lett*., **103**, 053903-1 (2009).